



# Epidemic model with seasonality for avian influenza waves in humans

Fátima E. Cruziniani<sup>1,a</sup>, Enrique C. Gabrick<sup>2</sup>, Ana L. R. Moraes<sup>2</sup>, Moises S. Santos<sup>3</sup>, Antonio M. Batista<sup>1,4,b</sup> , José Trobia<sup>4</sup>, Kelly C. Iarosz<sup>1,5</sup>, Iberê L. Caldas<sup>2</sup>, and Jürgen Kurths<sup>6,7</sup>

<sup>1</sup> Postgraduate Program in Sciences, State University of Ponta Grossa, Ponta Grossa 84030-900, PR, Brazil

<sup>2</sup> Physics Institute, University of São Paulo, São Paulo 05508-090, SP, Brazil

<sup>3</sup> Municipal Secretary of Education of Ponta Grossa, Municipal Government, Ponta Grossa 84030-320, PR, Brazil

<sup>4</sup> Department of Mathematics and Statistics, State University of Ponta Grossa, Ponta Grossa 84030-900, PR, Brazil

<sup>5</sup> University Center UNIFATEB, Telêmaco Borba 84266-010, PR, Brazil

<sup>6</sup> Potsdam Institute for Climate Impact Research, Potsdam 14473, Germany

<sup>7</sup> Department of Physics, Humboldt University Berlin, Berlin 12489, Germany

Received 12 August 2025 / Accepted 26 December 2025

© The Author(s) 2026

**Abstract** Control strategies and prevention of infectious illnesses are challenges faced by the healthcare systems. Infectious diseases are caused by organisms and can be transmitted through different ways, such as contact between individuals of the same species or interspecies (zoonotic diseases). One contagious viral disease is the avian influenza, known as bird flu, that infects wild birds, as well as domestic poultry. It can also contaminate some mammalian species and was detected in humans. Epidemiologic models have been used to study the transmission dynamics of bird flu. In this work, we analyse a model that describes the spread of a avian influenza from birds to humans. We consider a compartmental model in which the bird system is divided into susceptible and infected birds (SI), whilst the human system is separated into susceptible, infected and recovered (SIR). In addition, we substantially extend this model by including seasonal effects in the transmission rate of the system and investigate the behaviour of the model through the waves of infection. We uncover that depending on the parameters and initial conditions, the number of disease cases can be kept under control, as well as it is possible to observe even disease-free state. Our results show that the initial conditions play a crucial role in the number of avian influenza waves. Furthermore, we demonstrate that the seasonal forcing increases the infection numbers and induces a more complex dynamical behaviour.

## 1 Introduction

Infectious diseases are illnesses caused by organisms, e.g. parasites, bacteria or virus, and transmitted between hosts by means of various types of mechanisms [1]. Giardiasis [2] and tuberculosis [3] are examples of common infectious diseases caused by parasites and bacteria, respectively. There are many viral infections, such as viral hepatitis [4], that is a liver inflammation, and influenza viruses, that are responsible for contagious respiratory illness [5].

With regard to the spread, the infectious diseases can be transmitted by means of different routes, such as direct and indirect when there is or not physical contact, respectively [6]. Moreover, certain diseases can be spread by insects [7, 8], examples include dengue [9, 10], chikungunya [11], and malaria [12]. Various illnesses are spread to humans by contact with animals, such as rabies and toxoplasmosis. Rabies is a common and fatal infection associated with dogs bites and with bats [13]. Toxoplasmosis spreads from eating undercooked meat and contacting with cat faeces [14].

In 1878, Perroncito [15] reported the first description of the highly pathogenic avian influenza (HPAI). Centanni and Savonuzzi [16] identified in 1901 that HPAI is caused by a virus. Depending on the virus characteristic, the

<sup>a</sup> e-mail: [fatimaeliscruziniani@gmail.com](mailto:fatimaeliscruziniani@gmail.com)

<sup>b</sup> e-mail: [antoniomarcosbatista@gmail.com](mailto:antoniomarcosbatista@gmail.com) (corresponding author)

avian influenza is a contagious disease that can be either low or highly pathogenic [17]. The avian influenza can contaminate not only domestic and wild avian, but also mammalian species, including humans [18, 19]. The avian influenza type A viruses is divided into multiple subtypes according to the proteins on the virus surface, e.g. H5N1, H7N9 and H9N2. Since 1997 and 2013, H5N1 and H7N9, respectively, have killed millions of domesticated avian species and infected humans [20, 21]. Peiris et al. [22] published clinical features of cases of human infection with H9N2.

There are evidences of seasonal patterns of the avian influenza. The mechanisms that generate seasonality in the dynamical behaviour of the influenza have been investigated by Berry et al. [23]. Park and Glass [24] observed seasonal patterns of incidence of avian and human influenza in east and southeast Asia. Gonzales et al. [25] characterised seasonal patterns related to the avian influenza viruses introduced into free-range layer farms in the Netherlands. They verified that high risk period for introduction of low pathogenic avian influenza and abundance of migratory birds are correlated. Tian et al. [26] demonstrated an association between the timing of H5N1 and bird migration, as well as viral transmission networks in Asia.

Mathematical models in epidemiology have been proposed to describe the transmission and spread of infectious diseases [27–31]. In 1976, Larson et al. [32] introduced the first mathematical model for the within-host dynamics of an influenza infection. Malek and Hoque [33] developed a deterministic model of avian influenza with vaccination and treatment for the poultry farms. Considering a mathematical model, Derouich and Boutayeb [34] analysed the dynamic behaviour of human infection by avian influenza. They carried out simulations and stability analysis with different parameter values. Tuncer and Martcheva [35] considered seven models to investigate the mechanisms which drive the seasonality of H5N1 influenza.

In this work, we study an avian-human influenza model with a seasonal forcing. Our model describes the spread of the influenza from birds to humans. In humans, the avian influenza can cause different symptoms. It has been reported mild symptoms, such as headaches and fatigue, as well as severe symptoms, in particular pneumonia. It is divided into compartments, that are susceptible (S), infected (I) and recovered (R). Iwami et al. [36] constructed a SI–SIR model without seasonality to study the spread of avian influenza in humans. Tuncer and Martcheva [35] considered seasonality in a SI–SI model with transmission from birds to humans. Therefore, our work is a substantial extension of both papers because we propose a SI–SIR model with a seasonal forcing in the rate in which the birds evolve to be infected. The bird and human systems are given by the SI and SIR models, respectively. Including the R compartment in the human population, the modification introduces the possibility of immunity against the illness. The individuals are removed from the chain of infection. By seasonal forcing of the model parameters, the number of disease cases can be kept under control, as well as it is possible to observe disease-free regimes. We verify that the magnitude of the infection peak depends on the rates that birds and humans evolve to be infected. One of our main results is to show the resurgence of infection after the report of few cases, known as wave, due to the periodic time-dependent transmission rate. We find that the number of avian influenza waves depends not only on the parameters, but also on the initial conditions.

The paper is organised as follows. In Sect. 2, the model is presented in detail. In Sects. 3 and 4, numerical simulations about human infection with avian influenza considering the model without and with seasonality are discussed, respectively. Finally, Sect. 5 presents our conclusion.

## 2 Mathematical model

In this paper, the bird and human populations are governed by SI and SIR models, respectively, as represented in Fig. 1, where the dotted line shows the interaction between them. Humans can only become infected by avian influenza due to the contact with infected birds. Even with a high death rate, humans can still recover [37]. The virulence of this disease is higher for birds and, in consequence, the infected birds are dead or remain infected for the whole life.

The mathematical model is given by

$$\begin{aligned}
 \frac{dS_b}{dt} &= \nu - \rho S_b - \alpha S_b I_b, \\
 \frac{dI_b}{dt} &= \alpha S_b I_b - (\rho + \chi) I_b, \\
 \frac{dS_h}{dt} &= \lambda - \mu S_h - \beta S_h I_b, \\
 \frac{dI_h}{dt} &= \beta S_h I_b - (\mu + \delta + \gamma) I_h, \\
 \frac{dR_h}{dt} &= \gamma I_h - \mu R_h,
 \end{aligned} \tag{1}$$

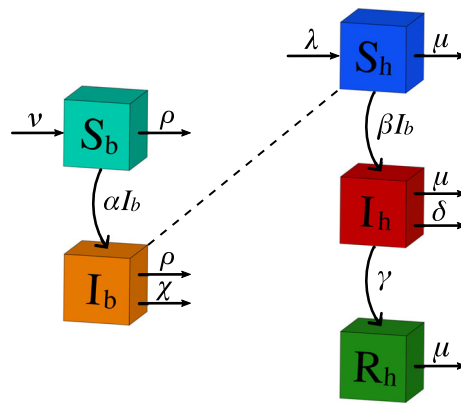


**Fig. 1** Compartment diagram of the SI–SIR model, where  $S_b$  and  $I_b$  are the number of the susceptible and infected bird populations, respectively,  $\nu$  is the rate in which the birds are born,  $\rho$  is the bird death rate,  $\alpha$  is the rate that the birds evolve to be infected, and  $\chi$  is the bird death rate due to avian influenza.  $S_h$ ,  $I_h$  and  $R_h$  are the number of susceptible, infected and recovered human populations, respectively,  $\lambda$  is the rate in which humans are born,  $\mu$  is the human death rate,  $\beta$  is the effective contact rate from birds to humans,  $\delta$  is the human death rate due to avian influenza, and  $\gamma$  is the rate in which the infected humans recover

**Table 1** Parameter values taken from the literature [35, 42]

Symbol	Meaning	Value (per day)
$\nu$	Bird natality rate	1020/365
$\rho$	Natural bird death rate	$1/(2 \times 365)$
$\chi$	Bird death rate due to HPAI	0.37
$\lambda$	Human natality rate	1000/365
$\mu$	Natural human death rate	$1/(73 \times 365)$
$\delta$	Human death rate due to HPAI	0.15
$\gamma$	Human recovery rate	0.2

where the population is divided into five compartments:  $S_b$  (susceptible birds),  $I_b$  (infected birds),  $S_h$  (susceptible humans),  $I_h$  (infected humans) and  $R_h$  (recovered humans).  $S_b$  and  $I_b$  are in units of  $10^7$  bird individuals, whilst  $S_h$ ,  $I_h$  and  $R_h$  are in units of  $10^5$  people. The parameter  $\nu$  corresponds to the rate in which the birds are born and  $\rho$  is the death rate of susceptible and infected birds. An additional death rate due to the avian influenza is given by  $\chi$ .  $\alpha$  is the rate that the birds evolve to be infected, and  $\lambda$  is the rate in which humans are born. The parameter  $\mu$  is related to the death rate of susceptible, infected and recovered humans. The parameter  $\beta$  is the effective contact rate of infective individuals. The parameters  $\delta$  and  $\gamma$  correspond to the human death rate due to HPAI and human recovery rate, respectively. Table 1 describes the parameter values taken from the cited references that we use in our simulations. Due to the fact that the risk of birds transmit avian influenza to humans to be low,  $\beta$  is much less than  $\alpha$ . According to Lucchetti et al. [38],  $\alpha$  is approximately equal to  $10^{-4}$ . Tuncer and Martcheva [35] suggested  $10^{-8} \leq \beta \leq 10^{-11}$ . A seasonal forcing is included in the transmission rate

$$\alpha(t) = \alpha_1 \sin[2\pi(t + \omega)] + \alpha_2, \tag{2}$$

where  $\alpha_1$ ,  $\alpha_2$  and  $\omega$  are the amplitude, vertical shift and phase shift, respectively [35, 39]. To ensure that  $\alpha(t) \geq 0$ , we assume  $\alpha_2 \geq \alpha_1$ . The sinusoidal function is a first approximation; however, it can represent a linear transformation of a weather covariate [40]. The advantage is the ease of interpretation and qualitative analysis.

### 3 Dynamical behaviour without seasonality

An essential way to start the analysis of the model (Eq. (1)) is through the investigation of the dynamical behaviour near the equilibrium solutions. Such solutions can be obtained by

$$\begin{aligned}
 \nu - \rho S_b - \alpha S_b I_b &= 0, \\
 \alpha S_b I_b - (\rho + \chi) I_b &= 0, \\
 \lambda - \mu S_h - \beta S_h I_b &= 0, \\
 \beta S_h I_b - (\mu + \delta + \gamma) I_h &= 0, \\
 \gamma I_h - \mu R_h &= 0,
 \end{aligned}
 \tag{3}$$

where  $\alpha$  is the rate that the birds evolve to be infected and  $\beta$  is the effective contact rate from birds to humans. Solving Eq. (3) for  $S_b, I_b, S_h, I_h$  and  $R_h$ , we find the equilibrium points. In epidemiological systems, we are interested in two forms of equilibria, the disease-free equilibrium, where there is no disease in the population, and the endemic equilibrium, where the disease persists in the population.

Considering  $I_b$  and  $I_h$  equals to zero, we find the disease-free equilibrium, given by

$$\begin{aligned}
 S_b &= \nu / \rho, \\
 I_b &= 0, \\
 S_h &= \lambda / \mu, \\
 I_h &= 0, \\
 R_h &= 0.
 \end{aligned}$$

A fundamental concept in the context of epidemiology is the basic reproductive number, generally denoted as  $R_0$ . It is defined as the number of secondary infectives per index case in a population of susceptibles [41]. In our model, when all birds are susceptible, we have  $S_b = \nu / \rho$ . The transmission rate of the disease is  $\alpha$ , and the lifetime of an infected bird is  $1 / (\rho + \chi)$ . Using the standard next-generation method, we compute  $R_0$  by means of

$$R_0 = a(FV^{-1}),
 \tag{4}$$

where

$$F = \begin{pmatrix} \frac{\alpha \nu}{\rho} & 0 \\ \frac{\beta \lambda}{\nu} & 0 \end{pmatrix},
 \tag{5}$$

$$V^{-1} = \begin{pmatrix} \frac{1}{\rho + \chi} & 0 \\ 0 & \frac{1}{\mu + \delta + \gamma} \end{pmatrix},
 \tag{6}$$

and  $a(A)$  is the spectral radius, that is defined as the maximum of the absolute values of the eigenvalues of  $A$ . Therefore,  $R_0$  for the bird population is determined as

$$R_0 = \frac{\alpha \nu}{(\rho + \chi) \rho}.$$

On the other hand, since no human can infect another individual in our model, there is no meaning for establishing a  $R_0$  for the human population.

Considering all populations greater than zero and solving Eq. (3), the endemic equilibrium is here given by

$$\begin{aligned}
 S_b^* &= \frac{\nu}{\rho} \frac{1}{R_0}, \\
 I_b^* &= \frac{\rho}{\alpha} (R_0 - 1), \\
 S_h^* &= \frac{\lambda}{\mu + \beta I_b^*}, \\
 I_h^* &= \frac{\beta S_h^* I_b^*}{\mu + \delta + \gamma}, \\
 R_h^* &= \frac{\gamma I_h^*}{\mu}.
 \end{aligned}$$

The stability of an equilibrium point is associated with the Jacobian matrix of the system. If the real part of all eigenvalues is less than zero, the stability is ensured. The Jacobian matrix is given by

$$\mathcal{J} = \begin{pmatrix} -\alpha I_b - \rho & -\alpha S_b & 0 & 0 & 0 \\ \alpha I_b & \alpha S_b - \rho - \chi & 0 & 0 & 0 \\ 0 & -\beta S_h & -\mu - \beta I_b & 0 & 0 \\ 0 & \beta S_h & \beta I_b & -\zeta & 0 \\ 0 & 0 & 0 & \gamma & -\mu \end{pmatrix},$$

where  $\zeta = \mu + \delta + \gamma$ . The characteristic polynomial of  $\mathcal{J}$  is

$$\det(\mathcal{J} - \Lambda \mathbb{I}) = [-(\alpha I_b + \rho + \Lambda)(\alpha S_b - \rho - \chi - \Lambda) + \alpha^2 S_b I_b](\mu + \beta I_b + \Lambda)(\zeta + \Lambda)(\mu + \Lambda). \tag{7}$$

Therefore, the eigenvalues of the system are

$$\begin{aligned} \Lambda_1 &= -\mu, \\ \Lambda_2 &= -\zeta, \\ \Lambda_3 &= -\mu - \beta I_b, \\ \Lambda_4 &= \frac{\alpha(S_b - I_b) - 2\rho - \chi + \sqrt{\Delta}}{2}, \\ \Lambda_5 &= \frac{\alpha(S_b - I_b) - 2\rho - \chi - \sqrt{\Delta}}{2}, \end{aligned}$$

where  $\Delta = \alpha^2(S_b^2 + I_b^2 - 2S_b I_b) - 2\alpha\chi(S_b + I_b) + \chi^2$ .

The eigenvalues of  $\mathcal{J}$  evaluated at the disease-free equilibrium are

$$\begin{aligned} \Lambda_1 &= -\mu, \\ \Lambda_2 &= -\zeta, \\ \Lambda_3 &= -\mu, \\ \Lambda_4 &= \alpha\nu/\rho - \rho - \chi, \\ \Lambda_5 &= -\rho. \end{aligned}$$

The stable disease-free equilibrium occurs when  $\Lambda_4 < 0$ , which yields  $\alpha < \rho(\rho + \chi)/\nu$  ( $R_0 < 1$ ), where  $\alpha$  is the rate that the birds evolve to be infected. The equilibrium becomes unstable when  $\Lambda_4 > 0$ , which yields  $\alpha > \rho(\rho + \chi)/\nu$  ( $R_0 > 1$ ).

The eigenvalues of  $\mathcal{J}$  evaluated at the endemic equilibrium are

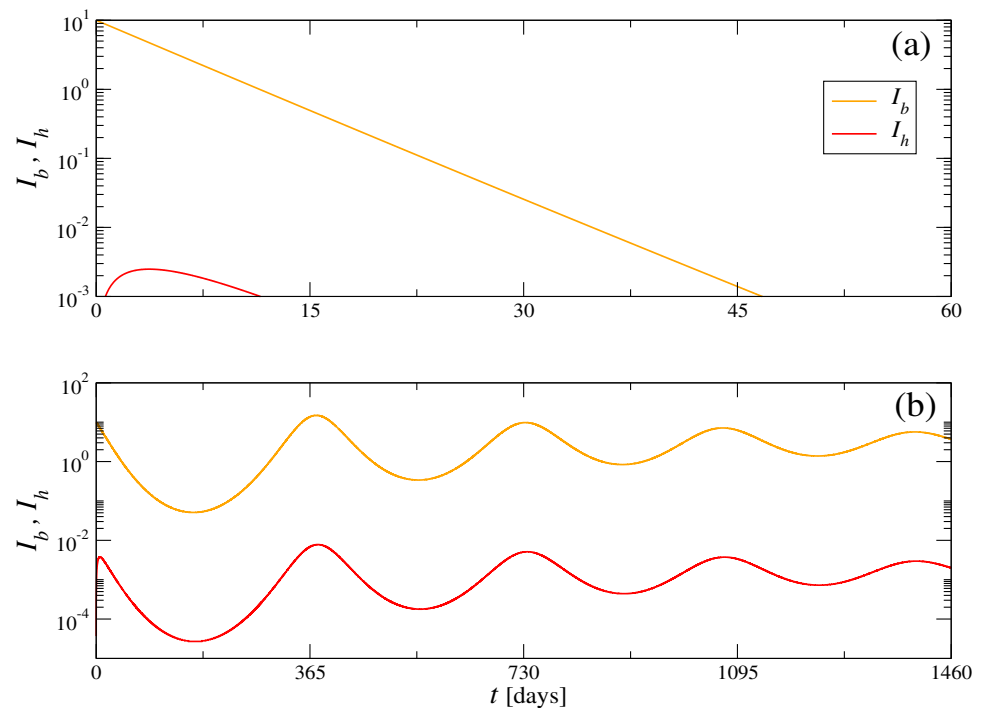
$$\begin{aligned} \Lambda_1 &= -\mu - \beta I_b^*, \\ \Lambda_2 &= -\mu - \delta - \gamma, \\ \Lambda_3 &= -\mu, \\ \Lambda_4 &= -\frac{\rho R_0}{2} + \frac{\sqrt{\Delta}}{2}, \\ \Lambda_5 &= -\frac{\rho R_0}{2} - \frac{\sqrt{\Delta}}{2}, \end{aligned}$$

where  $\Delta = (\rho R_0)^2 - 4\rho(\chi + \rho)(R_0 - 1)$ . If  $\Delta < 0$ , the endemic equilibrium is a stable focus. The state variables  $I_b$  and  $S_b$  reach an equilibrium through damped oscillations with period  $T = 2\pi/\sqrt{\Delta}$ .

It is worth mentioning that we searched for chaotic solutions within the range of parameters described in Table 1, but none were found. Furthermore, in the first model presented by Tuncer and Martcheva [35], there is chaotic solution, for an SI-SI seasonal model. Selecting the same parameters set as Tuncer and Martcheva, our model preserves the chaotic orbit for  $\gamma = 0.1$ .

First, we analyse the time evolution of the populations without considering the seasonal forcing effects. We verify that different solutions are possible by changing the values of the parameters. In Fig. 2a, for  $\alpha = 1.7 \times 10^{-4}$  (the rate that the birds evolve to be infected) and  $\beta = 2.3 \times 10^{-9}$  (the effective contact rate from birds to humans),

**Fig. 2** Time evolution of the infected birds ( $I_b$ ) and infected humans ( $I_h$ ) populations in orange and red lines, respectively. We consider  $\beta = 2.3 \times 10^{-9}$ ,  $\alpha = 1.7 \times 10^{-4}$  in **a** and  $\alpha = 3.2 \times 10^{-4}$  in **b**, where  $\alpha$  is the rate that the birds evolve to be infected and  $\beta$  is the effective contact rate of infective individuals. The initial conditions are given by  $S_b(0) = 10^3$ ,  $I_b(0) = 10$ ,  $S_h(0) = 8 \times 10^4$ ,  $I_h(0) = 0$ , and  $R_h(0) = 0$ . For  $t$  greater than 4000 days in the panel **(b)**,  $I_b$  and  $I_h$  go to steady points, corresponding to endemic solutions.  $S_b$  and  $I_b$  are in units of  $10^7$  bird individuals, whilst  $S_h$ ,  $I_h$  and  $R_h$  are in units of  $10^5$  people



we observe a disease-free solution, where the populations of infected individuals are extinguished after a time period. In this case, once  $R_0 = 0.93$ . For  $\alpha = 3.2 \times 10^{-4}$  and  $\beta = 2.3 \times 10^{-9}$ , which corresponds to  $R_0 = 1.76$ , we see that the infected bird and human populations do not go to zero, as well as the avian influenza does not disappear, as displayed in Fig. 2b, characterising an endemic solution.

We compute the parameter space  $\alpha \times \beta$  for the maximum number of infected humans ( $I_{h_{\max}}$ ) in a time interval equal to 4 years and a transient time equal to 2 months, as shown in Fig. 3. The colour bar corresponds to the values of  $I_{h_{\max}}$ . For  $\alpha < 10^{-4}$ , there is a non-significant number of infected humans. This occurs due to the fact that, in this region, the  $R_0$  value is close to 1. For  $\alpha = 1.8 \times 10^{-4}$  we get  $R_0 = 1$ , highlighted by the vertical dotted white line. Increasing  $\alpha$  and  $\beta$ , we observe that the avian influenza spreads from birds to humans. For  $\alpha < 4 \times 10^{-4}$ ,  $I_{h_{\max}}$  does not depend on  $\beta$ . In the range  $R_0 < 1$ , there is no success in the disease invasion. Therefore, depending on  $\alpha$ , it can be observed not only a disease-free, but also an endemic solution. According to our simulations,  $\alpha$  plays an important role in the maximum number of infected humans.

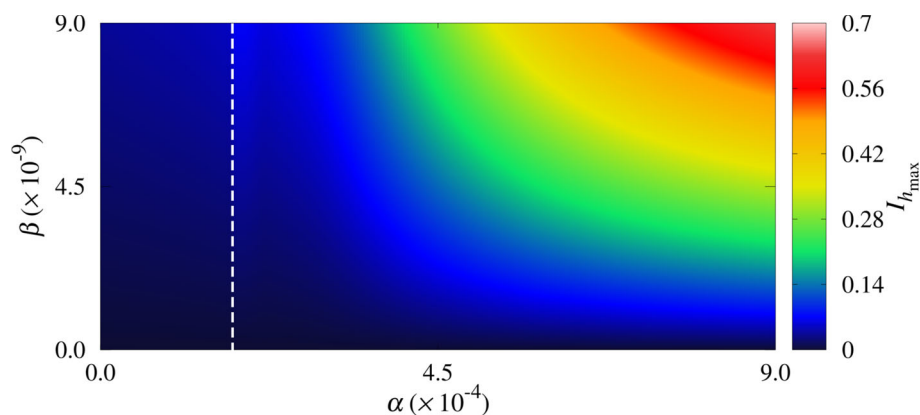


**Fig. 3** Parameter space of the effective contact rate of infective individuals versus the rate that the birds evolve to be infected ( $\beta \times \alpha$ ) for  $S_b(0) = 10^3$ ,  $I_b(0) = 40$ ,  $S_h(0) = 8 \times 10^4$ ,  $I_h(0) = 0$ , and  $R_h(0) = 0$ . The colour bar corresponds to the maximum number of infected humans ( $I_{h_{\max}}$ ). For  $\alpha < 1.8 \times 10^{-4}$ , there is a non-significant number of infected humans. This occurs due to the fact that  $\alpha = 1.8 \times 10^{-4}$  defines the threshold  $R_0 = 1$  (white dashed line).  $S_b$  and  $I_b$  are in units of  $10^7$  bird individuals, whilst  $S_h$ ,  $I_h$  and  $R_h$  are in units of  $10^5$  people

### 4 Dynamical behaviour with seasonality

Seasonal cycle of diseases has been identified in many viral infections, for instance influenza. There has been studies about the seasonality of avian influenza waves. Potdar et al. [43] reported a human case of avian influenza in India, coinciding with the monsoon season in India. Seasonal behaviour was also observed in poultry outbreaks in Indonesia, Egypt and Vietnam [35].

We introduce now a seasonal forcing according to Eq. (2) and investigate the dynamical behaviour of the avian influenza model given by Eq. (1). Considering a time-dependent transmission rate  $\alpha(t)$ , the basic reproduction number can also vary with the time in the form  $R_0(t) \propto \alpha(t)$ . The transmission rate  $\alpha(t)$  achieves a maximum value when  $\sin[2\pi(t + \omega)] = 1$ , i.e.  $\alpha_{\max} = \alpha_1 + \alpha_2$ , where  $\alpha_1$  is the amplitude and  $\alpha_2$  is the vertical shift of the transmission rate related to the seasonal forcing. The minimum value occurs when  $\sin[2\pi(t + \omega)] = -1$ , i.e.  $\alpha_{\min} = \alpha_1 - \alpha_2$ . Therefore, due to the condition  $\alpha_1 \leq \alpha_2$ , the maximum ( $R_0^+$ ) and the minimum ( $R_0^-$ ) basic reproduction numbers are given by

$$R_0^\pm = \frac{(\alpha_2 \pm \alpha_1)\nu}{(\rho + \chi)\rho}. \tag{8}$$

Calculating the derivative of the fourth equation in Eq. (1), we get

$$\frac{d^2 I_h}{dt^2} + (\mu + \delta + \gamma) \frac{dI_h}{dt} = F(\beta, S_h, I_b, \dot{S}_h, \dot{I}_b). \tag{9}$$

Depending on the parameters, the differential equation can exhibit oscillating solutions, namely waves of infection. In addition, these oscillations are sustained by the external forcing that appears in  $F(\cdot)$ .

In the peak wave, the first derivative is equal to zero. Setting the fourth equation in Eq. (1) equal to zero, we obtain

$$I_h = \frac{\beta}{\mu + \delta + \gamma} S_h I_b. \tag{10}$$

By means of the third equation, we get

$$S_h I_b = \frac{1}{\beta} \left( -\frac{dS_h}{dt} - \mu S_h + \lambda \right), \tag{11}$$

that gives

$$I_h = \frac{1}{\mu + \delta + \gamma} \left( -\frac{dS_h}{dt} - \mu S_h + \lambda \right). \tag{12}$$

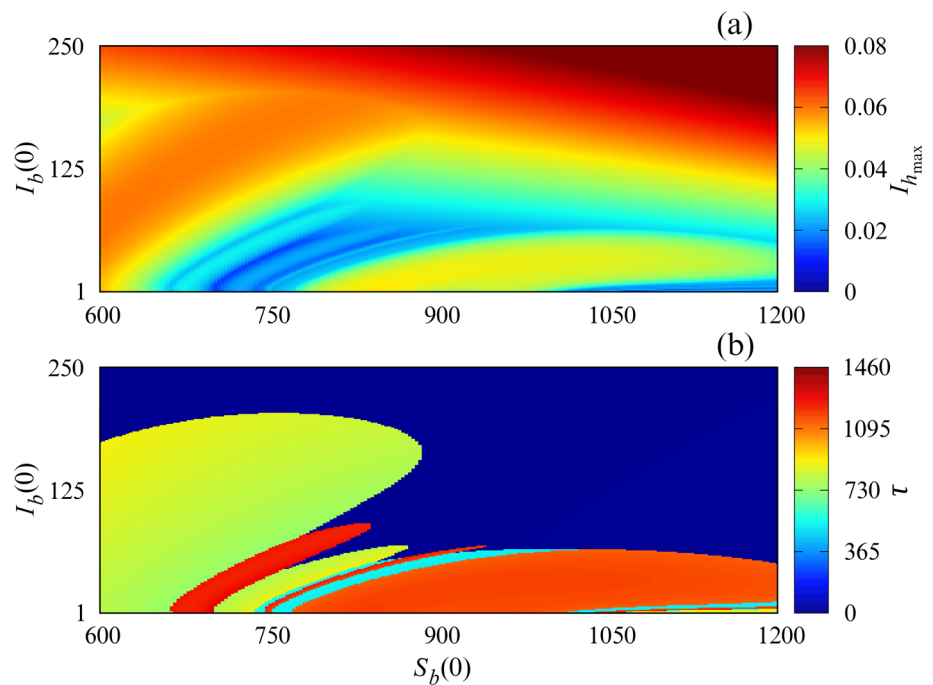
The differential equation inside the parentheses has an exponential solution. Therefore, for the parameters considered in this work, the peak values decay exponentially.

In Fig. 4, we vary the initial conditions  $I_b(0)$  and  $S_b(0)$  for  $S_h(0) = 8 \times 10^4$ ,  $I_h(0) = 0$ , and  $R_h(0) = 0$ , considering 4 years and a transient time equal to 2 months. Figure 4a displays  $I_{h_{\max}}$  in the colour bar from 0 to 0.08. The dark blue regions show the initial conditions related to the birds in which the maximum number of infected humans is non-significant. In the red regions, the avian influenza infects a higher number of humans. In Fig. 4b, we plot the day ( $\tau$ ) on which the  $I_{h_{\max}}$  occurs. The blue and red regions exhibit the smaller and higher values of  $\tau$ . Depending on the initial conditions, it is possible to see that a high value of  $I_{h_{\max}}$  can appear in a short time.

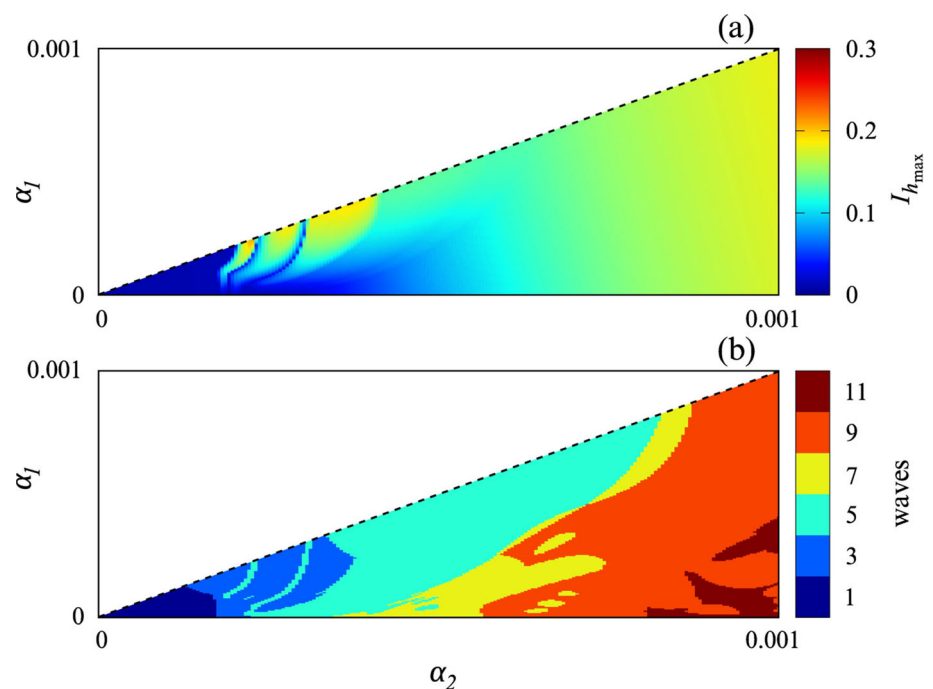
Figure 4 shows the existence of a subset of initial conditions in the phase space, known as basin of attraction, that leads the trajectories to  $I_{h_{\max}} > 0.07$ , as displayed in the panel (a). The topological structure is not trivial and the basin boundaries are smooth. Comparing the panels (a) and (b), the  $\tau$  value is small for a large subset of initial conditions, mainly for  $I_{h_{\max}} > 0.07$ .

We compute the parameter space  $\alpha_1 \times \alpha_2$  for  $S_b(0) = 10^3$ ,  $I_b(0) = 40$ ,  $S_h(0) = 8 \times 10^4$ ,  $I_h(0) = 0$ ,  $R_h(0) = 0$ ,  $\beta = 2.3 \times 10^{-9}$  (the effective contact rate of infective individuals), and  $\omega = 0.9707$ , as displayed in Fig. 5. The white colour corresponds to the forbidden region, i.e.  $\alpha_1 > \alpha_2$ . In Fig. 5a, the red regions exhibit  $I_{h_{\max}} \approx 0.3$ , whilst the blue regions show values close to 0 for small  $\alpha_2$ . Figure 5b displays the amount of avian influenza waves in humans (colour bar), namely the number of epidemic peaks in a time interval equal to 4 years. A wave indicates that the number of infected individuals is rising, namely there is a defined peak and then a decline. The number of infection waves in humans is based on the local maximum values of  $I_h$ . The local maximum is defined as the

**Fig. 4**  $I_b(0) \times S_b(0)$  for  $S_h(0) = 8 \times 10^4$ ,  $I_h(0) = 0$ , and  $R_h(0) = 0$ . The colour bars correspond to  $I_{h_{\max}}$  and  $\tau$  in the panels (a) and (b), respectively. We consider  $\beta = 2.3 \times 10^{-9}$  (the effective contact rate from birds to humans) and  $\alpha$  (the rate that the birds evolve to be infected) varying with time according to Eq. (2), where  $\alpha_1 = 5.11 \times 10^{-5}$ ,  $\alpha_2 = 3.26 \times 10^{-4}$ , and  $\omega = 0.9707$ .  $S_b$  and  $I_b$  are in units of  $10^7$  bird individuals, whilst  $S_h$ ,  $I_h$  and  $R_h$  are in units of  $10^5$  people



**Fig. 5** Parameter space  $\alpha_1 \times \alpha_2$  for  $S_b(0) = 10^3$ ,  $I_b(0) = 40$ ,  $S_h(0) = 8 \times 10^4$ ,  $I_h(0) = 0$ , and  $R_h(0) = 0$ . We consider  $\beta = 2.3 \times 10^{-9}$  (the effective contact rate of infective individuals) and  $\omega = 0.9707$ . The colour bars correspond to  $I_{h_{\max}}$  and the amount of waves in the panels (a) and (b), respectively. For  $\alpha_1 > \alpha_2$  (white region), prohibited region.  $S_b$  and  $I_b$  are in units of  $10^7$  bird individuals, whilst  $S_h$ ,  $I_h$  and  $R_h$  are in units of  $10^5$  people



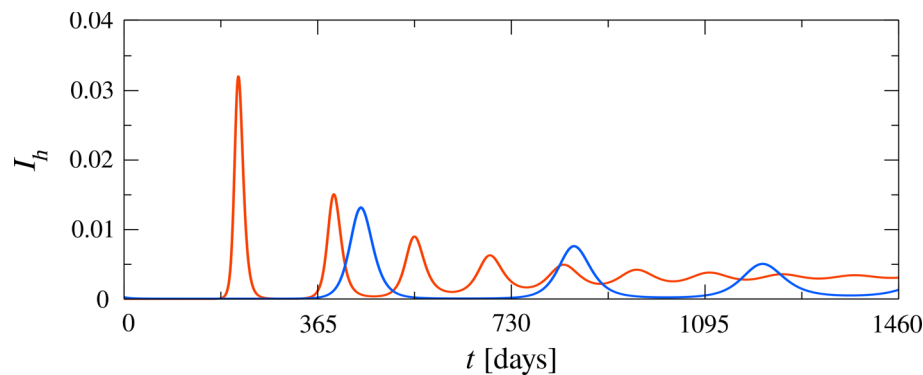
greatest value within a given interval time. The number of waves corresponds to the quantity of local maximum  $I_h$  in 4 years.

Figure 6 displays three and nine waves in blue ( $\alpha_1 = 2.2 \times 10^{-4}$  and  $\alpha_2 = 3.2 \times 10^{-4}$ ) and orange ( $\alpha_1 = 1.6 \times 10^{-4}$  and  $\alpha_2 = 9.4 \times 10^{-4}$ ) colours, respectively, according to Fig. 5b. The patterns are composed of peaks and valleys. Increasing  $\alpha_2$ , we find that the amount of waves increases.

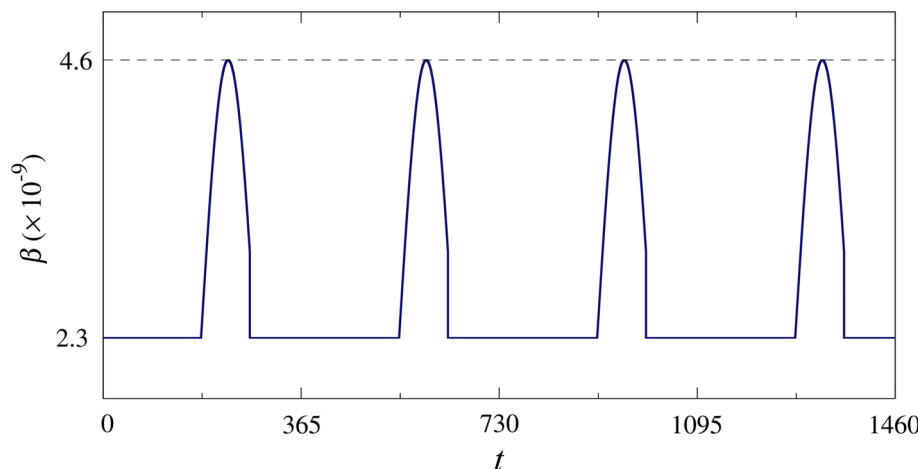
Figure 5 displays a significant dependence of  $I_{h_{\max}}$  and the amount of waves on  $\alpha_2$ . Computing the parameter values ( $\alpha_1$  and  $\alpha_2$ ) and observing the changes in the behaviour of the solutions, we verify the appearance of fixed points. We again do not find chaotic behaviour in the range of the considered parameters.

We propose a periodic variation on  $\beta$  (the effective contact rate from birds to humans) that increases from  $2.3 \times 10^{-9}$  to  $4.6 \times 10^{-9}$  during the winter, as displayed in Fig. 7. With a seasonal forcing in  $\alpha$  (the rate that

**Fig. 6** Time evolution of  $I_h$  for  $\alpha_1 = 2.2 \times 10^{-4}$  and  $\alpha_2 = 3.2 \times 10^{-4}$  showing three waves (blue line) and for  $\alpha_1 = 1.6 \times 10^{-4}$  and  $\alpha_2 = 9.4 \times 10^{-4}$  exhibiting nine waves (orange line) in a time interval equal to 4 years.  $S_b$  and  $I_b$  are in units of  $10^7$  bird individuals, whilst  $S_h$ ,  $I_h$  and  $R_h$  are in units of  $10^5$  people



**Fig. 7** Temporal evolution of  $\beta$  (the effective contact rate from birds to humans) considering  $\beta = 2.3 \times 10^{-9}[1 + \epsilon \sin(2\pi\Omega t)]$ , where  $\Omega = 5 \times 10^{-4}$  and  $\epsilon$  equal to 1 (winter) or 0 (other seasons)



the birds evolve to be infected) and a variation in  $\beta$ , we calculate the amount of waves as a function of the initial conditions related to the susceptible and infected bird populations.

Figure 8a and b displays the waves as a function of  $I_b(0)$  and  $S_b(0)$  for  $\beta = 2.3 \times 10^{-9}$  and  $\beta$  (the effective contact rate from birds to humans) increasing in the winters, respectively. We consider  $S_h(0) = 8 \times 10^4$ ,  $I_h(0) = 0$ , and  $R_h(0) = 0$ . Comparing Fig. 8a with 8b, we see that the amount of waves increases when a small change in  $\beta$  during the winter is considered. The orange and red regions that are associated with 4 and 5 waves, respectively, have a considerable increase.

In Fig. 8, we identify subsets of initial conditions, namely basins of attraction, in which the solutions tend to different amount of waves. Hence, they are different attractors with smooth basin boundaries. The seasonality plays an important role in the basin structure.

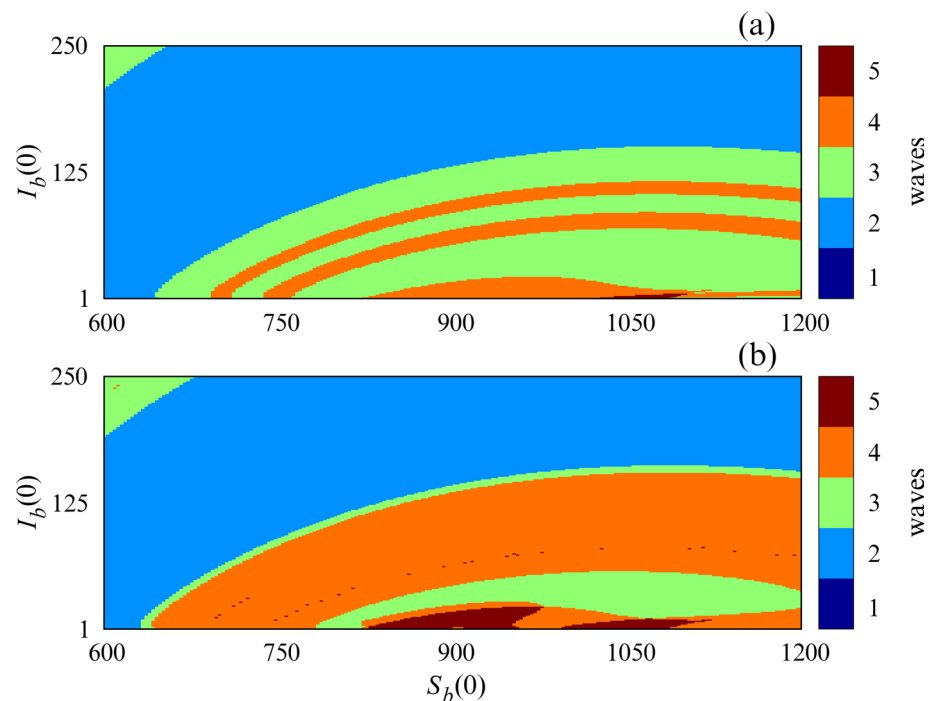
In our simulations, we verify the dependence of the maximum number of infected humans on the initial conditions related to the birds. The amount of waves in humans also depends on the initial conditions. By varying  $\alpha_1$  and  $\alpha_2$ , we observe changes in  $I_{h_{max}}$  and in the amount of waves.

## 5 Conclusion

Infectious diseases are illnesses caused by pathogens, such as viruses and bacteria. They can be spread between individual from the same or different species. The flu is an example of common infectious diseases caused by viruses. The avian influenza, also known as bird flu, spread amongst wild birds and domestic poultry, and can also be transmitted to some mammalian species, including humans.

In this work, we study a seasonal avian-human influenza epidemic model. It is a compartmental model composed of bird and human systems. The bird system is separated into susceptible and infected birds (SI model), whereas the human system is divided into susceptible, infected and removed individuals (SIR model). We include a seasonality in the effective contact rate of infective humans. We consider parameter values from the World Health Organisation [42]. Our results are in agreement with the number of cases of H5N1 avian influenza in birds and humans collected in Indonesia and the rest of the World reported by Tuncer et al. [35].

**Fig. 8**  $I_b(0) \times S_b(0)$  for  $S_h(0) = 8 \times 10^4$ ,  $I_h(0) = 0$ , and  $R_h(0) = 0$ . The colour bar corresponds to the amount of waves. We consider  $\beta = 2.3 \times 10^{-9}$  in the panel (a) and  $\beta(t)$  varying according to Fig. 7 in the panel (b).  $S_b$  and  $I_b$  are in units of  $10^7$  bird individuals, whilst  $S_h$ ,  $I_h$ , and  $R_h$  are in units of  $10^5$  people



Without seasonality, the maximum number of infected humans depends not only on the effective contact rate from birds to humans, but also on the rate that the birds evolve to be infected. It is possible to observe disease-free, as well as the situation in which the disease is endemic, namely the infectious is constantly present.

Considering a seasonal forcing in the rate that the birds evolve to be infected, we compute the maximum number of infected humans ( $I_{h_{\max}}$ ) and avian influenza waves in humans. By varying the initial conditions related to the susceptible and infected bird populations, we mainly find that a high number of infected humans can appear in a short time. The amount of waves increases when a small increase in the effective contact rate from birds to humans during the winter is considered. In this work, we show that the initial conditions and the parameters related to the bird populations play an important role in the transmission of avian influenza from birds to humans. All in all, the seasonal forced model has significant infection numbers and a more complex dynamical behaviour than the infected one.

Instead of using a SI–SI model, we choose one SI–SIR, once the humans are infected and acquire immunity against an illness. The SI–SI model is adequate when the individuals become sick for the whole life. If the individuals cannot be reinfected, similar conclusions can be obtained in the SI–SI model.

The existence of basin of attraction was shown by Yakubu and Ziyadi [44] in a zoonotic infectious disease model with demographic strong Allee effect. They studied the Feline immunodeficiency virus that is responsible for the AIDS in cat populations. We find basin of attraction in which the initial conditions can lead to different amount of waves. Recently, seasonal waves of pathogenic avian influenza were reported in Japan and South Korea [45].

Concerning the epidemiological aspects, confirmed human cases of avian influenza in China from 2013 to 2017 were analysed by Artois and collaborators [46]. Tadmon and collaborators [47] proposed a two-strain avian-human influenza model. The human-to-human transmissions occur due to an avian influenza virus strain. The existence and stability of equilibrium points were studied. They demonstrated that the quarantine of infected humans can be a control strategy of transmissions. In future works, we plan to include infected humans with the mutant strain.

Our results contribute to show that the initial condition estimation can improve the precision of epidemic modelling related to avian influenza waves in humans, supporting more effective public health policies.

**Acknowledgements** The authors would like to thank the financial support from the Brazilian Federal Agencies: CNPq (Grant 304616/2021-4), CAPES, Fundação Araucária, and FAPESP (Grants 2024/05700-5, 2025/02318-5, and 2025/05453-0). E.C.G. thanks the financial support from Coordenação de Aperfeiçoamento de Pessoal de Nível Superior - Brasil (CAPES) - Finance Code 88881.846051/2023-01. We would like to thank URL: [www.105groupscience.com](http://www.105groupscience.com).

**Funding** The Article Processing Charge (APC) for the publication of this research was funded by the Coordenação de Aperfeiçoamento de Pessoal de Nível Superior - Brasil (CAPES) (ROR identifier: 00x0ma614).

**Data Availability** The data that support the findings of this study are openly available in Zenodo at <https://doi.org/10.5281/zenodo.17992598> and in Github at [https://github.com/ecgabrick/Seasonal\\_avian\\_flu\\_model](https://github.com/ecgabrick/Seasonal_avian_flu_model).

**Open Access** This article is licensed under a Creative Commons Attribution 4.0 International License, which permits use, sharing, adaptation, distribution and reproduction in any medium or format, as long as you give appropriate credit to the original author(s) and the source, provide a link to the Creative Commons licence, and indicate if changes were made. The images or other third party material in this article are included in the article's Creative Commons licence, unless indicated otherwise in a credit line to the material. If material is not included in the article's Creative Commons licence and your intended use is not permitted by statutory regulation or exceeds the permitted use, you will need to obtain permission directly from the copyright holder. To view a copy of this licence, visit <http://creativecommons.org/licenses/by/4.0/>.

## References

1. S. Funk, M. Salathé, V.A.A. Jansen, Modeling the influence of human behaviour on the spread of infectious diseases: A review. *J. R. Soc. Interface* **7**, 1247–1256 (2010)
2. E.A. Meyer, E.L. Jarroll, Giardiasis. *Am. J. Epidemiol.* **111**, 1–12 (1980)
3. J.L. Flynn, J. Chan, Immunology of tuberculosis. *Annu. Rev. Immunol.* **19**, 93–129 (2001)
4. L.G. Guidotti, F.V. Chisari, Immunobiology and pathogenesis of viral hepatitis. *Annu. Rev. Pathol.: Mech. Dis.* **1**, 23–61 (2006)
5. N.M. Bouvier, P. Palese, The biology of influenza viruses. *Vaccine* **26S**, D49–D53 (2008)
6. J.A. Drewe, H.M. O'Connor, N. Weber, R.A. McDonald, R.J. Delahay, Patterns of direct and indirect contact between cattle and badgers naturally infected with tuberculosis. *Epidemiol. Infect.* **141**, 1467–1475 (2013)
7. L.A. Moreira, I. Iturbe-Ormaetxe, J.A. Jeffery, G. Lu, A.T. Pyke, L.M. Hedges, B.C. Rocha, S. Hall-Mendelin, A. Day, M. Riegler, L.E. Hugo, K.N. Johnson, B.H. Kay, E.A. McGraw, A.F. van den Hurk, P.A. Ryan, S.L. O'Neill, A Wolbachia symbiont in *Aedes aegypti* limits infection with dengue, Chikungunya and Plasmodium. *Cell* **139**, 1268–1278 (2009)
8. G. Bian, D. Joshi, Y. Dong, P. Lu, G. Zhou, X. Pan, Y. Xu, G. Dimopoulos, Z. Xi, Wolbachia invades *Anopheles stephensi* populations and induces refractoriness to Plasmodium infection. *Science* **340**, 748–751 (2013)
9. S. Bhatt, P.W. Gething, O.J. Brady, J.P. Messina, A.W. Farlow, C.L. Moyes, J.M. Drake, J.S. Brownstein, A.G. Hoen, O. Sankoh, M.F. Myers, D.B. George, T. Jaenisch, G.R.W. Wint, C.P. Simmons, T.W. Scott, J.J. Farrar, S.I. Hay, The global distribution and burden of dengue. *Nature* **496**, 504–507 (2013)
10. S.T. Silva, E.C. Gabrick, P.R. Protachevicz, K.C. Iarosz, I.L. Caldas, A.M. Batista, J. Kurths, When climate variables improve the dengue forecasting: a machine learning approach. *The European Physical Special Topics* (2024). <https://doi.org/10.1140/epjs/s11734-024-01201-7>
11. G. Pialoux, B.A. Gaüzère, S. Jauréguiberry, M. Strobel, Chikungunya, an epidemic arbovirosis. *Lancet Infect. Dis.* **7**, 319–327 (2007)
12. J. Oliveira-Ferreira, M.V.G. Lacerda, P. Brasil, J.L.B. Ladislau, P.L. Taulil, C.T. Daniel-Ribeiro, Malaria in Brazil: an overview. *Malar. J.* **9**, 115 (2010)
13. T. Hemachudha, G. Ugolini, S. Wacharapluesadee, W. Sungkarat, S. Shuangshoti, J. Laothamatas, Human rabies: Neuropathogenesis, diagnosis, and management. *Lancet Neurol.* **12**, 498–513 (2013)
14. L.M. Weiss, J.P. Dubey, Toxoplasmosis: A history of clinical observations. *Int. J. Parasitol.* **39**, 895–901 (2009)
15. E. Perroncito, Epizoozia tifoide nei gallinacei. *Annali. Accad. Agri. Torino* **21**, 87–126 (1878)
16. E. Centanni, E. Savonuzzi, La peste aviaria I & II. Comunicazione fatta all'accademia delle scienze mediche e naturali de Ferrara (1901)
17. D.J. Alexander, An overview of the epidemiology of avian influenza. *Vaccine* **25**, 5637–5644 (2007)
18. B. Lupiani, S.M. Reddy, The history of avian influenza. *Comp. Immunol. Microbiol. Infect. Dis.* **32**, 311–323 (2009)
19. N.R.S. Martins, An overview on avian influenza. *Braz. J. Poult. Sci.* **14**, 71–158 (2012)
20. K. Dhama, S. Chakraborty, R. Tiwari, A. Kumar, A. Rahal, S.K. Latheef, M.Y. Wani, S. Kapoor, Avian/bird flu virus: Poultry pathogen having zoonotic and pandemic threats: A review. *J. Med. Sci.* **13**, 301–315 (2013)
21. Y. Poovorawan, S. Pyungporn, S. Prachayangprecha, J. Makkoch, Global alert to avian influenza virus infection: From H5N1 to H7N9. *Pathog. Glob. Health* **107**, 217–223 (2013)
22. M. Peiris, K.Y. Yuen, C.W. Leung, K.H. Chan, P.L.S. Ip, R.W.M. Lai, W.K. Orr, K.F. Shortridge, Human infection with influenza H9N2. *Lancet* **354**, 916–917 (1999)
23. I. Berry, M. Rahman, M.S. Flora, T. Shirin, A.S.M. Alamgir, M.H. Khan, R. Anwar, M. Lisa, F. Chowdhury, M.A. Islam, M.G. Osmani, S. Dunkle, E. Brum, A.L. Greer, S.K. Morris, P. Mangtani, D.N. Fisman, Seasonality of influenza and coseasonality with avian influenza in Bangladesh, 2010–19: A retrospective, time-series analysis. *Lancet Glob. Health* **10**, e1150–e1158 (2022)
24. A.W. Park, K. Glass, Dynamic patterns of avian and human influenza in east and southeast Asia. *Lancet Infect. Dis.* **7**, 543–548 (2007)
25. J.L. Gonzales, S. Pritz-Verschuren, R. Bouwstra, J. Wiegel, A.R.W. Elbers, N. Beerens, Seasonal risk of low pathogenic avian influenza virus introductions into free-range layer farms in the Netherlands. *Transbound. Emerg. Dis.* **68**, 127–136 (2021)

26. H. Tian, S. Zhou, L. Dong, T.P.V. Boeckel, Y. Cui, S.H. Newman, J.Y. Takekawa, D.J. Prosser, X. Xiao, Y. Wu, B. Cazelles, S. Huang, R. Yang, B.T. Grenfell, B. Xu, Avian influenza H5N1 viral and bird migration networks in Asia. *PNAS* **112**, 172–177 (2015)
27. A.M. Batista, S.L.T. Souza, K.C. Iarosz, A.C.L. Almeida, J.D. Szezech Jr., E.C. Gabrick, M. Mugnaine, G.L. Santos, I.L. Caldas, Simulation of deterministic compartmental models for infectious diseases dynamics. *Rev. Bras. Ensino Fis.* **43**, e20210171 (2021)
28. T. Tomé, A.T.C. Silva, M.J. de Oliveira, Effect of immunization through vaccination on deterministic models for epidemic spreading. *Braz. J. Phys.* **51**, 1853 (2021)
29. T. Tomé, M.J. de Oliveira, Effect of immunization through vaccination on the SIS epidemic spreading model. *J. Phys. A* **55**, 275602 (2022)
30. E.C. Gabrick, P.R. Protachevicz, A.M. Batista, K.C. Iarosz, S.L.T. Souza, A.C.L. Almeida, J.D. Szezech Jr., M. Mugnaine, I.L. Caldas, Effect of two vaccine doses in the SEIR epidemic model using a stochastic cellular automaton. *Physica A* **597**, 127258 (2022)
31. M. Mugnaine, E.C. Gabrick, P.R. Protachevicz, K.C. Iarosz, S.L.T. Souza, A.C.L. Almeida, A.M. Batista, I.L. Caldas, J.D. Szezech Jr., R.L. Viana, Control attenuation and temporary immunity in a cellular automata SEIR epidemic model. *Chaos Soliton. Fract.* **155**, 111784 (2022)
32. E. Larson, J. Dominik, A. Rowberg, G. Higbee, Influenza virus population dynamics in the respiratory tract of experimentally infected mice. *Infect. Immun.* **13**, 438–447 (1976)
33. A. Malek, A. Hoque, Mathematical modeling of bird flu with vaccination and treatment for the poultry farms. *Comp. Immunol. Microbiol. Infect. Dis.* **80**, 101721 (2022)
34. M. Derouich, A. Boutayeb, An avian influenza mathematical model. *Appl. Math. Sci.* **2**, 1749–1760 (2008)
35. N. Tuncer, M. Martcheva, Modeling seasonality in avian influenza H5N1. *J. Biol. Syst.* **21**, 1340004 (2013)
36. S. Iwami, Y. Takeuchi, X. Liu, Avian-human influenza epidemic model. *Math. Biosci.* **207**, 1–25 (2007)
37. L. Alexakis, H. Buczkowski, M. Ducatex, A. Fusaro, J.L. Gonzales, T. Kuiken, K. Stahl, C. Staubach, O. Svartström, C. Terregino, K. Willgert, R. Delacourt, L. Kohnle, Avian influenza overview June–September 2024. *EFSA J.* **22**, 9057 (2024)
38. J. Lucchetti, M. Roy, M. Martcheva, An avian influenza model and its fit to human avian influenza cases. *Advances in Disease Epidemiology* **1**, 1–30 (2009)
39. E.C. Gabrick, E. Sayari, P.R. Protachevicz, J.D. Szezech Jr., K.C. Iarosz, S.L.T. de Souza, A.C.L. Almeida, R.L. Viana, I.L. Caldas, A.M. Batista, Unpredictability in seasonal infectious diseases spread. *Chaos Solit. Fractals* **166**, 113001 (2023)
40. J.M. Ponciano, M.A. Capistrán, First principles modeling of nonlinear incidence rates in seasonal epidemics. *PLoS Comput. Biol.* **7**, e1001079 (2011)
41. M.J. Keeling, P. Rohani, Modeling infectious diseases in humans and animals. Princeton University Press (2008)
42. <https://www.who.int/data/gho/data/themes/mortality-and-global-health-estimates/ghe-life-expectancy-and-healthy-life-expectancy>
43. V. Potdar, M. Brijwal, R. Lodha, P. Yadav, S. Jadhav, M.L. Choudhary, A. Choudhary, V. Vipat, N. Gupta, A.K. Deorari, L. Dar, P. Abraham, Identification of human case of avian influenza A(H5N1) infection. *India. Emerg. Infect. Dis.* **28**, 1269–1273 (2022)
44. A.-A. Yakubu, N. Ziyadi, Stong Allee effect and basins of attraction in a discrete-time zoonotic infectious disease model. *Nat. Resour. Model.* **35**, e12310 (2022)
45. L.J. Kjaer, C.T. Kirkeby, A.E. Boklund, C.K. Hjulsager, A.D. Fox, M.P. Ward, Prediction model show differences in highly pathogenic avian influenza outbreaks in Japan and South Korea compared to Europe. *Sci. Rep.* **15**, 6783 (2025)
46. J. Artois, H. Jiang, X. Wang, Y. Qin, M. Percy, S. Lai, Y. Shi, J. Zhang, Z. Peng, J. Zheng, Y. He, M.S. Dhingra, S. von Dobschuetz, F. Guo, V. Martin, W. Kalpravidh, F. Claes, T. Robinson, S.I. Hay, X. Xiao, L. Feng, M. Gilbert, H. Yu, Changing geographic patterns and risk factors for avian influenza A (H7N9) infections in humans. *China. Emerg. Infect. Dis.* **24**, 87–94 (2018)
47. C. Tadmon, A.F. Fossi, B. Tsanou, A two-strain avian-influenza model with environmental transmissions: Stability analysis and optimal control strategies. *Commun. Nonlinear Sci. Simulat.* **133**, 107981 (2024)